Stability of the Liquid-Fluidized Magnetically Stabilized Fluidized Bed

Conan J. Fee
Bioprocess Technology Section, Meat Industry Research Institute of New Zealand
Centre for Technology, University of Waikato, Hamilton, New Zealand

Rosensweig's (1979) analysis of the stability of gas-fluidized magnetically stabilized fluidized beds (MSFBs) with voidage perturbations is modified to include terms dependent on the fluid density. This allows the stability analysis to be applicable to liquid-fluidized MSFBs, which have potential use in liquid chromatography. Results show that in systems where the fluid density is not insignificant when compared to the solid-phase density, the difference in density between the two phases should be used when normalizing the magnetization required to achieve stability. Comparisons between theory and experiment show that although the present analysis improves on Rosensweig's analysis, it still does not give reliable, quantitative predictions of stability behavior. It is suggested that for liquid-fluidized MSFBs, stability to particle velocity perturbations, rather than to voidage perturbations, is more relevant to chromatographic applications wherein the purpose of magnetic stabilization is to prevent particle mixing as opposed to preventing the occurrence of bubbling and slugging observed in gas-fluidized beds.

Introduction

In column chromatography, fluidized beds offer advantages over packed beds in that they operate with axial pressure drops that are virtually independent of superficial velocities and they can tolerate solids in the feedstream without blocking. However, if more than a single separation stage is required, then superficial velocities must be close to the minimum fluidization velocity to minimize axial mixing of bed particles caused by voidage instabilities. Magnetic stabilization can suppress solids phase mixing and thus extend the range of useful operation to higher superficial velocities (Rosensweig, 1979). The magnetically stabilized fluidized bed (MSFB) has a further advantage for chromatographic applications in that when bed particles are withdrawn continuously from the bottom of the column, the MSFB can be operated in a continuous, countercurrent mode due to the downward plug flow of the solids phase through the column (Burns et al., 1985).

Graves (1993) outlined several reasons why MSFB chromatography has not yet been widely adopted, the most significant being a lack of suitable magnetically susceptible chromatographic beads. Beads produced in individual laboratories (Burns et al., 1985; Lochmüller et al., 1987; Goetz et al., 1991), while possessing excellent fluidization and stabilization characteristics, have various drawbacks that limit their industrial use (Graves, 1993). Commercially available magnetic beads are generally designed for mix-and-recover systems and have too low a density with their very small sizes to be useful in MSFBs (Graves, 1993). A poly-acrylamide-magnetite (PAM) bead has recently been developed that shows a good range of stability in an MSFB at superficial velocities similar to those used in conventional high-performance liquid chromatography (HPLC) (Cocker, 1994), despite the material having a much lower density (1,200 kg/m^3) than the materials used by workers just cited (>1,700 kg/m^3). Therefore, for a bead to be used in an MSFB, it need not necessarily have a high density.

It would be advantageous to be able to predict the stability ranges of new resins when assessing their potential usefulness. Moreover, it would be useful to be able to predict ranges of stability in liquid-fluidized MSFB systems from theory rather than to rely solely on experimentally determined values, as this would enable an algorithm to be developed for controlling magnetic field strength as a function of throughput rate for a particular column and resin combination. Such

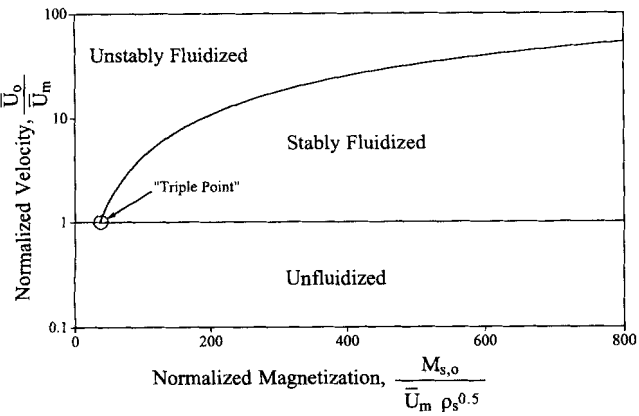

Figure 1. Topology of the MSFB stability diagram (Rosensweig, 1979).

an algorithm would, in turn, simplify the use of MSFB technology and thus overcome another of the barriers to its acceptance as a processing tool.

Rosensweig (1979) studied the magnetic stabilization of the fluidized state of gas-fluidized beds. He showed a boundary between stability and instability, with respect to voidage perturbations, in a plot of normalized superficial velocity against normalized magnetization of the bed particles. The plot (Figure 1) contained three regions: the unfluidized bed; the stabilized fluidized bed; and the unstabilized ("bubbling") fluidized bed. The topology of the plot was likened to that of a physical chemical phase diagram, with the three regions being analagous to regions of solid, liquid, and vapor phases, respectively. A "triple point" was identified where the boundary between the stabilized and unstabilized regions joined with the boundary between the fluidized and unfluidized regions. Such a topology has been shown to occur experimentally (Siegell, 1991).

Rosensweig considered only gas-fluidized MSFBs, so could neglect fluid density in comparison with particle densities. However, in liquid-fluidized MSFBs the fluid density cannot be neglected, so the normalized magnetization term given by Rosensweig is not applicable. Thus, Rosensweig's analysis does not show how solids densities that approach liquid phase densities might affect magnetic stabilization. Rosensweig and Ciprios (1991) studied liquid-fluidized MSFBs, but neglected virtual mass and concentrated mainly on the case of fluidization of nonmagnetic spheres with a magnetic ferrofluid, for which they found reasonable agreement between theory and experiment. However, this system is unlikely to be of significant value to protein chromatography because of the sensitivity of proteins to their environment. Furthermore, they did not develop a normalized magnetization term corresponding to that of Rosensweig (1979). Intuitively, one might expect the solids density term in Rosensweig's analysis of the normalized magnetization to be replaced by the difference in density between solids and liquid phases, in which case stability would require an increasing magnetic field strength with decreasing density difference.

In the present article, Rosensweig's analysis is extended to include terms dependent on fluid density, and it is shown that the normalized magnetization term should indeed contain the difference between solids and fluid phase densities. A comparison between the resultant theory and experimentally determined ranges of stable operation shows that the theory still cannot be used to quantitatively predict magnetic stabilization ranges.

Basic Relationships

Equations 1 to 4 are the same as those used by Anderson and Jackson (1968) for analyzing the stability of conventional fluidized beds, except a magnetic stress tensor term is added in the particle equation of motion (Eq. 4). This is the approach used by Rosensweig (1979), except that here the terms in fluid density in Eq. 3 are not neglected. The equations of continuity are therefore, for the fluid phase,

$$\frac{\partial \epsilon}{\partial t} + \nabla\cdot(\epsilon \boldsymbol{u}) = 0, \tag{1}$$

and, for the particles,

$$\frac{\partial (1-\epsilon)}{\partial t} + \nabla\cdot((1-\epsilon)\boldsymbol{v}) = 0. \tag{2}$$

The equations of motion are, for the fluid,

$$\rho_f \epsilon \left[\frac{\partial \boldsymbol{u}}{\partial t} + (\boldsymbol{u}\cdot\nabla)\boldsymbol{u}\right] = \epsilon\nabla\cdot\boldsymbol{E} - \boldsymbol{f} + \epsilon\rho_f \boldsymbol{g}, \tag{3}$$

and, for the particles,

$$(1-\epsilon)\rho_s \left[\frac{\partial \boldsymbol{v}}{\partial t} + (\boldsymbol{v}\cdot\nabla)\boldsymbol{v}\right] = (1-\epsilon)\nabla\cdot\boldsymbol{E} + \boldsymbol{f} + (1-\epsilon)\rho_s \boldsymbol{g} + \nabla\cdot\boldsymbol{E}^s + \nabla\cdot\boldsymbol{E}^m. \tag{4}$$

From Maxwell's equations, the magnetostatic field equations are (Rosensweig, 1979),

$$\text{curl } \boldsymbol{H} = 0 \tag{5}$$

$$\text{div } \boldsymbol{B} = 0 \tag{6}$$

$$\boldsymbol{B} = \boldsymbol{M} + \mu_o \boldsymbol{H} \tag{7}$$

Constitutive Relationships

The constitutive relationships between $\boldsymbol{f}$, $\boldsymbol{E}$, $\boldsymbol{E}^s$, $\boldsymbol{E}^m$, and $\boldsymbol{M}$ are as follows:

1. Fluid–particle interaction term:

$$\boldsymbol{f} = \epsilon\beta(\epsilon, \boldsymbol{M})(\boldsymbol{u}-\boldsymbol{v}) + (1-\epsilon)C(\epsilon)\rho_f \frac{\partial}{\partial t}(\boldsymbol{u}-\boldsymbol{v}), \tag{8}$$

where $C(\epsilon)$ is a virtual mass coefficient to be defined later.

2. Fluid stress tensor:

$$\nabla\cdot\boldsymbol{E} = -\nabla p. \tag{9}$$

3. Solids stress tensor:

$$\nabla \cdot \boldsymbol{E}^s = 0. \tag{10}$$

4. Magnetic stress tensor:

$$\nabla \cdot \boldsymbol{E}^m = \boldsymbol{f}_m = (\boldsymbol{M} \cdot \nabla)\boldsymbol{H} = M \nabla H. \tag{11}$$

The magnetic equation of state, as defined by Rosensweig (1979), is

$$\frac{\boldsymbol{M}}{M_s} = (1-\epsilon)\frac{\boldsymbol{H}}{H}. \tag{12}$$

Two additional terms that will be required later for consideration of the perturbation of the magnetization vector are the chord susceptibility and the tangent susceptibility, given by Eqs. 13 and 14:

$$\text{Chord susceptibility} = \chi_o = \frac{M_{s,o}}{H_o} \tag{13}$$

$$\text{Tangent susceptibility} = \hat{\chi} = \left(\frac{\partial M_{s,o}}{\partial H}\right)_{H_o}. \tag{14}$$

Solution for Steady State with Uniform Magnetic Field

The steady-state solution with a uniform magnetic field is one in which the velocity of the particles is everywhere zero and the voidage is constant. Under these circumstances

$$\begin{aligned} \boldsymbol{u} &= \boldsymbol{u}_o = i u_o \\ \boldsymbol{v} &= \boldsymbol{v}_o = 0 \\ \epsilon &= \epsilon_o \\ \boldsymbol{H} &= \boldsymbol{H}_o = \boldsymbol{i}_o H_o \\ \boldsymbol{M} &= \boldsymbol{M}_o = \boldsymbol{i}_o M_o \\ \boldsymbol{B} &= \boldsymbol{B}_o = \boldsymbol{i}_o B_o, \end{aligned} \tag{15}$$

where $\boldsymbol{i}$ is the unit vector in the upward direction, $\boldsymbol{i}_o$ is a unit vector in the direction of the applied field, and u_o, ϵ_o, H_o, and M_o are constants. Equations 15 satisfy the continuity and magnetostatic field equations, Eqs. 1 and 2, identically, while the fluid equation of motion equation, Eq. 3, reduces to

$$\nabla p_o + \beta(\epsilon_o) u_o \boldsymbol{i} = 0. \tag{16}$$

When Eq. 16 is combined with Eq. 3 of motion for the solids to eliminate p_o, the result is, recognizing that $\boldsymbol{g} = -g\boldsymbol{i}$ and grad $H_o = 0$,

$$\beta_o u_o - g(1-\epsilon_o)(\rho_s - \rho_f) = 0, \tag{17}$$

where β_o is the value of $\beta(\epsilon)$ at $\epsilon = \epsilon_o$. Equations 16 and 17 therefore show that the imposition of the magnetic field has no effect on the steady-state solution.

Stability of the Steady-State Solution

We now investigate the stability of the steady-state solution. The following perturbations are introduced to the steady-state solution in the usual manner:

$$\begin{aligned} \boldsymbol{u} &= \boldsymbol{u}_o + \boldsymbol{u}_1 = i u_o + \boldsymbol{u}_1 \\ \boldsymbol{v} &= \boldsymbol{v}_o + \boldsymbol{v}_1 = \boldsymbol{v}_1 \\ \epsilon &= \epsilon_o + \epsilon_1 \\ p &= p_o + p_1 \\ \boldsymbol{H} &= \boldsymbol{H}_o + \boldsymbol{H}_1 = \boldsymbol{i}_o H_o + \boldsymbol{H}_1 \\ \boldsymbol{M} &= \boldsymbol{M}_o + \boldsymbol{M}_1 = \boldsymbol{i}_o M_o + \boldsymbol{M}_1 \\ \boldsymbol{B} &= \boldsymbol{B}_o + \boldsymbol{B}_1 = \boldsymbol{i}_o B_o + \boldsymbol{B}_1. \end{aligned} \tag{18}$$

Introducing the perturbations into Eqs. 1 to 4, neglecting second-order terms in small quantities, and combining them with Eqs. 9, 10, 11 and the steady-state solution (Eq. 17), we obtain from Eq. 1

$$\frac{\partial \epsilon_1}{\partial t} + \epsilon_o \nabla \cdot \boldsymbol{u}_1 + i u_o \nabla \epsilon_1 = 0, \tag{1'}$$

from Eq. 2

$$-\frac{\partial \epsilon_1}{\partial t} + (1-\epsilon_o)\nabla \cdot \boldsymbol{v}_1 = 0, \tag{2'}$$

and from Eq. 3

$$\begin{aligned} \rho_f \epsilon_o \left[\frac{\partial \boldsymbol{u}_1}{\partial t} + (i u_o \cdot \nabla)\boldsymbol{u}_1\right] = &-\epsilon_o \nabla p_1 - \epsilon_1 \beta_o u_o \boldsymbol{i} \\ &- \epsilon_o \epsilon_1 \beta_o' u_o \boldsymbol{i} - \epsilon_o \beta_o (\boldsymbol{u}_1 - \boldsymbol{v}_1) \\ &-(1-\epsilon_o) C_o \rho_f \frac{\partial}{\partial t}(\boldsymbol{u}_1 - \boldsymbol{v}_1) + (\epsilon_o + \epsilon_1)\rho_f \boldsymbol{g}, \end{aligned} \tag{3'}$$

where β_o' and C_o' are $\partial\beta/\partial\epsilon\,|_{\epsilon=\epsilon_o+\epsilon_1}$ and $\partial C/\partial\epsilon\,|_{\epsilon=\epsilon_o+\epsilon_1}$, respectively. Equation 3′ can be used to eliminate grad (p_1) in obtaining Eq. 4′:

$$\begin{aligned} (1-\epsilon_o)\rho_s \frac{\partial \boldsymbol{v}_1}{\partial t} = &(1-\epsilon_o)\rho_f \left[\frac{\partial \boldsymbol{u}_1}{\partial t} + (i u_o \cdot \nabla)\boldsymbol{u}_1\right] \\ &+ \left[1 + \frac{\epsilon_1}{\epsilon_o} + \epsilon_1 \frac{\beta_o'}{\beta_o} + \frac{(\boldsymbol{u}_1 - \boldsymbol{v}_1)}{u_o}\right](1-\epsilon_o)(\rho_s - \rho_f)\boldsymbol{g} \\ &+ \frac{(1-\epsilon_o)}{\epsilon_o} C_o \rho_f \frac{\partial}{\partial t}(\boldsymbol{u}_1 - \boldsymbol{v}_1) + (1-\epsilon_o-\epsilon_1)(\rho_s - \rho_f)\boldsymbol{g} \\ &- \frac{\epsilon_1}{\epsilon_o}\rho_f \boldsymbol{g} + M_{s,o} \nabla(\boldsymbol{H}_i \boldsymbol{i}_o). \end{aligned} \tag{4'}$$

Taking the divergence of Eq. 4′, we obtain a partial differential in the voidage perturbation ϵ_1. In obtaining this we substitute for div $\boldsymbol{u}_1$ and div $\boldsymbol{v}_1$ from Eqs. 1′ and 2′, and eliminate β_o using the steady state equation, Eq. 17:

$$\left[\rho_s+\frac{(1-\epsilon_o)}{\epsilon_o}\rho_f+\frac{C_o\rho_f}{\epsilon_o^2}\right]\frac{\partial^2\epsilon_1}{\partial t^2}+\frac{(\rho_s-\rho_f)}{\epsilon_o u_o}g\frac{\partial\epsilon_1}{\partial t}$$
$$+\left[\left(2+\frac{C_o}{\epsilon_o}\right)\left(\frac{1-\epsilon_o}{\epsilon_o}\right)u_o\rho_f\right]\frac{\partial^2\epsilon_1}{\partial t\partial x}+\left(\frac{1-\epsilon_o}{\epsilon_o}\right)u_o^2\rho_f\frac{\partial^2\epsilon_1}{\partial x^2}$$
$$+\left[\frac{(1-\epsilon_o)}{\epsilon_o}(\rho_s-\rho_f)g-g\rho_s-g(1-\epsilon_o)(\rho_s-\rho_f)\frac{\beta_o'}{\beta_o}\right.$$
$$\left.+\rho_f g\frac{(\epsilon_o-1)}{\epsilon_o}\right]\frac{\partial\epsilon_1}{\partial x}-\alpha(1-\epsilon_o)M_{s,o}^2\nabla^2\epsilon_1=0, \quad (19)$$

where

$$\alpha=\frac{\cos^2\theta}{1+(1-\epsilon_o)(1-\cos^2\theta)\chi_o+\hat{\chi}(1-\epsilon_o)\cos^2\theta}, \quad (20)$$

where θ is the angle between the applied field vector $\boldsymbol{H}_o$ and the wave vector number $\boldsymbol{k}$. The angle between the direction of the unperturbed flow and the wave vector is taken to be zero to give the greatest sensitivity to instabilities (Rosensweig, 1979). Dividing Eq. 19 by $(\rho_s-\rho_f)$:

$$\left[\frac{\rho_s}{(\rho_s-\rho_f)}+\frac{(1-\epsilon_o)}{\epsilon_o}\frac{\rho_f}{(\rho_s-\rho_f)}+\frac{C_o}{\epsilon_o^2}\frac{\rho_f}{(\rho_s-\rho_f)}\right]\frac{\partial^2\epsilon_1}{\partial t^2}$$
$$+\frac{g}{\epsilon_o u_o}\frac{\partial\epsilon_1}{\partial t}+\left[\left(2+\frac{C_o}{\epsilon_o}\right)\frac{(1-\epsilon_o)}{\epsilon_o}\frac{\rho_f}{(\rho_s-\rho_f)}u_o\right]\frac{\partial^2\epsilon_1}{\partial t\partial x}$$
$$+\left[\frac{(1-\epsilon_o)}{\epsilon_o}\frac{\rho_f}{(\rho_s-\rho_f)}u_o^2\right]\frac{\partial^2\epsilon_1}{\partial x^2}+\left[g\frac{(1-\epsilon_o)}{\epsilon_o}\right.$$
$$\left.-\frac{g\rho_s}{(\rho_s-\rho_f)}-\frac{\beta_o'}{\beta_o}(1-\epsilon_o)g+\frac{\rho_f}{(\rho_s-\rho_f)}\frac{(\epsilon_o-1)}{\epsilon_o}g\right]\frac{\partial\epsilon_1}{\partial x}$$
$$-\alpha(1-\epsilon_o)\frac{M_{s,o}^2}{(\rho_s-\rho_f)}\nabla^2\epsilon_1=0. \quad (21)$$

We now seek plane wave solutions to Eq. 21 in the form:

$$\boldsymbol{u}_1=\hat{u}_1\exp(st)\exp(i\boldsymbol{kx})$$
$$\boldsymbol{v}_1=\hat{v}_1\exp(st)\exp(i\boldsymbol{kx})$$
$$\epsilon_1=\hat{\epsilon}_1\exp(st)\exp(i\boldsymbol{kx})$$
$$p_1=\hat{p}_1\exp(st)\exp(i\boldsymbol{kx}), \quad (22)$$

where the $\hat{}$ symbol denotes a vector amplitude or an amplitude, i is the square root of -1, $\boldsymbol{k}$ is a wave vector number, and $\boldsymbol{x}$ is a position vector. From these we find that

$$\frac{\partial^2\epsilon_1}{\partial t^2}=s^2\hat{\epsilon}_1\exp(st)\exp(i\boldsymbol{kx})$$
$$\frac{\partial\epsilon_1}{\partial t}=s\hat{\epsilon}_1\exp(st)\exp(i\boldsymbol{kx})$$
$$\frac{\partial^2\epsilon_1}{\partial x\partial t}=i^2\boldsymbol{k}^2\hat{\epsilon}_1\exp(st)\exp(i\boldsymbol{kx})$$
$$\frac{\partial\epsilon_1}{\partial x}=i\boldsymbol{k}\hat{\epsilon}_1\exp(st)\exp(i\boldsymbol{kx})$$
$$\frac{\partial^2\epsilon_1}{\partial x^2}=i^2\boldsymbol{k}^2\hat{\epsilon}_1\exp(st)\exp(i\boldsymbol{kx})$$
$$\nabla^2\epsilon_1=i^2\boldsymbol{k}^2\hat{\epsilon}_1\exp(st)\exp(i\boldsymbol{kx}). \quad (23)$$

Finally, we substitute from Equations 23 for the differential terms in Eq. 21 and multiply by $\epsilon_o/(1-\epsilon_o)$ to obtain the following quadratic in the complex frequency, s:

$$\hat{\epsilon}_1\left[\left[\frac{\rho_f}{(\rho_s-\rho_f)}+\frac{\epsilon_o}{(1-\epsilon_o)}\frac{\rho_s}{(\rho_s-\rho_f)}+\frac{C_o}{\epsilon_o(1-\epsilon_o)}\frac{\rho_f}{(\rho_s-\rho_f)}\right]s^2+\left[\frac{g}{(1-\epsilon_o)u_o}+\frac{\rho_f}{(\rho_s-\rho_f)}u_o\left(2+\frac{C_o}{\epsilon_o}\right)i\boldsymbol{k}\right]s\right.$$
$$\left.+\left[\epsilon_o\alpha\frac{M_{s,o}^2}{(\rho_s-\rho_f)}-\frac{\rho_f}{(\rho_s-\rho_f)}u_o^2\right]|\boldsymbol{k}|^2-\left[\frac{\epsilon_o}{(1-\epsilon_o)}g+\frac{g}{(1-\epsilon_o)}\frac{\rho_f}{(\rho_s-\rho_f)}+\epsilon_o\frac{\beta_o'}{\beta_o}g\right]i\boldsymbol{k}\right]=0. \quad (24)$$

For Eq. 24 to hold, either ϵ_1 is 0 or

$$As^2+(P+ibQ)s+(f-Db^2-ibPF)=0, \quad (25)$$

where

$$A=\left[\frac{\epsilon_o}{(1-\epsilon_o)}\frac{\rho_s}{(\rho_s-\rho_f)}+\frac{\rho_f}{(\rho_s-\rho_f)}+\frac{C_o}{\epsilon_o(1-\epsilon_o)}\frac{\rho_f}{(\rho_s-\rho_f)}\right] \quad (26)$$

$$P=\frac{g}{(1-\epsilon_o)u_o} \quad (27)$$

$$Q=\left(2+\frac{C_o}{\epsilon_o}\right)\frac{\rho_f}{(\rho_s-\rho_f)} \quad (28)$$

$$D=\frac{\rho_f}{(\rho_s-\rho_f)} \quad (29)$$

$$F=(1-\epsilon_o)\times\left[-1+\frac{\rho_s}{(\rho_s-\rho_f)}\left(\frac{\epsilon_o}{(1-\epsilon_o)}\right)+\epsilon_o\frac{\beta_o'}{\beta_o}+\frac{\rho_f}{(\rho_s-\rho_f)}\right] \quad (30)$$

$$b=u_o k \quad (31)$$

$$f = \alpha \frac{\epsilon_o M_{s,o}^2}{(\rho_s - \rho_f)} k^2. \tag{32}$$

In accordance with Rosensweig (1979), the value of θ is set to zero in deriving Eqs. 31 and 32 to give the solutions the greatest sensitivity to instabilities. We now use the Carman–Kozeny relation

$$\beta_o = \frac{K(1-\epsilon_o)^2}{\epsilon_o^2} \tag{33}$$

from which we find

$$\frac{\beta_o}{\beta_o'} = \frac{2}{\epsilon_o(1-\epsilon_o)} \tag{34}$$

as well as the superficial velocity $\bar{u}_o = \epsilon_o u_o$, to modify the preceding expressions for P, F, and b to give

$$P = \frac{g\epsilon_o}{(1-\epsilon_o)\bar{u}_o} \tag{27'}$$

$$F = \left[-3 + \epsilon_o + \frac{\rho_s}{(\rho_s - \rho_f)}\epsilon_o + \frac{\rho_f}{(\rho_s - \rho_f)}(1-\epsilon_o) \right] \tag{30'}$$

$$b = \frac{\bar{u}_o}{\epsilon_o} k. \tag{31'}$$

We can now seek the roots of Eq. 24. These have the following forms where the real roots are

$$\zeta = \frac{P}{2A}\left[-1 \pm \sqrt{\frac{[(1-z)^2 + q^2]^{1/2} + (1-z)}{2}} \right] \tag{35}$$

and the imaginary roots are

$$\eta = \frac{P}{2A}\left[-1 \pm \sqrt{\frac{[(1-z)^2 + q^2]^{1/2} - (1-z)}{2}} \right], \tag{36}$$

where

$$z = 4A\left(\frac{b}{P}\right)^2\left[\frac{Q^2}{4A} + \frac{f}{b^2} - D\right] \tag{37}$$

and

$$q = \frac{4AbF}{P} + \frac{2bQ}{P}. \tag{38}$$

Magnetic stabilization occurs if $\zeta < 0$ and neutral stability occurs when $\zeta = 0$. Accordingly, for neutral stability:

$$z = \frac{1}{4}q^2 \tag{39}$$

or, substituting from Eqs. 37 and 38 for z and q into Eq. 39, we obtain

$$\frac{f}{b^2} = [AF^2 + QF + D] \tag{40}$$

or

$$[AF^2 + QF + D]\left[\frac{b^2}{f}\right] = 1 \text{ for neutral stability.} \tag{41}$$

The condition of neutral stability can be written

$$N_m N_v = 1, \tag{42}$$

where

$$N_m = \frac{(\rho_s - \rho_f)\bar{u}_o^2}{M_{s,o}^2} \tag{43}$$

and

$$N_v = \frac{1}{\alpha\epsilon_o^3}[AF^2 + QF + D]. \tag{44}$$

Therefore,

$$N_v = \frac{1}{\epsilon_o^3}[AF^2 + QF + D][1 + (1-\epsilon_o)\hat{\chi}]. \tag{45}$$

Using the Carman–Kozeny equation and the steady-state solution in Eq. 17, we obtain

$$\frac{\bar{u}_o}{\bar{u}_m} = \frac{\epsilon_o^3}{(1-\epsilon_o)} \frac{(1-\epsilon_d)}{\epsilon_d^3}, \tag{46}$$

where $\bar{u}_m$ is the superficial velocity at minimum fluidizing conditions, where the voidage is merely equal to the "rest" or "dumped" solids voidage ϵ_d.

The normalized velocity can now be computed from Eq. 46, and for each value computed, the value of the normalized magnetization is given by Eq. 47:

$$\frac{M_{s,o}}{(\rho_s - \rho_f)^{1/2}\bar{u}_m} = N_v^{1/2}\frac{\bar{u}_o}{\bar{u}_m}. \tag{47}$$

Results and Discussion

The analysis shows that the proper term for normalized magnetization for MSFBs in which the density of the fluid is not vanishingly less than that of the solids phase includes the density difference between solids and fluid phases. When the fluid density is set to zero, the equations collapse to the equivalent expressions in Rosensweig's (1979) analysis. The solution also approaches that of Rosensweig as the solids phase density increases relative to the fluid density.

The effect of the solids phase density on the normalized magnetization required for stability is shown in Figure 2 for the case where fluid density is 1,000 kg/m^3. As expected, stabilization becomes exponentially more difficult as the solids phase density approaches that of the fluid phase. A minimum magnetization required for stability occurs in the range 1,600 to 1,900 kg/m^3. Coincidentally, this is in the range of densities of rehydrated calcium alginate/magnetite (CAM) beads (Cocker, 1994; Sacj et al., 1994).

Figure 3 shows a plot of normalized velocity against normalized magnetization for CAM beads fluidized in water. The value of the virtual mass coefficient is taken to be 0.5, the value usually associated with a single spherical particle falling through a fluid. The theoretical stability curve underesti-

mates stability, but lies quite close to the experimentally determined values of Cocker (1994), particularly at the higher superficial velocities. The theoretical stability curve is expected to be conservative in the absence of a solids stress tensor and under the assumption that the disturbance wave is oriented in the direction of flow. Also, the experimental technique used (Cocker, 1994) allowed observation of instabilities only near the outer surfaces of the bed. Instabilities within the bed itself would not have been noted.

The experimental data do not exhibit the so-called "triple point" for either the CAM beads or the PAM beads (Figure 4). (Note that a log scale is used on the horizontal axis of Figure 4 so that the theoretical curves are not obscured by the scale.) Although the theoretical curve calculated from Eqs. 46 and 47 is closer to the experimental points than that of Rosensweig (1979), there is still considerable difference between predicted and observed values.

The very high value of the normalized magnetization required for stabilization of the PAM beads may be misleading in that it may imply that PAM beads are considerably more difficult to stabilize than CAM beads. In fact, the applied magnetic field used to stabilize the PAM beads was of the same magnitude as that used for the CAM beads (Cocker, 1994). The experimentally determined value of the normalized magnetization is high due to the very low superficial velocity required for minimum fluidization of the PAM beads (3.5×10^{-5} m/s). Equation 47, however, does not contain terms directly dependent on the minimum fluidization velocity. The analysis is therefore insensitive to both particle size and fluid viscosity, on which minimum fluidization is dependent, and therefore the theory as it stands cannot be used to quantitatively predict bed stability.

The question as to what constitutes stability in the liquid-fluidized MSFB was recently brought to the author's attention (Tien,1993). In gas-fluidized systems, bubbling and slugging can be suppressed by magnetic stabilization. However, bubbling and slugging are not normally observed in the liquid-fluidized bed, and voidage remains essentially uniform on the macroscopic scale (Richardson and Zaki, 1954). Does it therefore make sense to carry out an analysis of stability with respect to voidage perturbations of the uniform fluidized state? Mixing of particles (particularly turbulent mixing) requires that they be moving independently of one another, with different velocities at different positions within the column. Since voidage is dependent on velocity, there must also be variations in voidage throughout the column if mixing is to occur, so mixing and voidage instabilities are linked. However, we are not concerned here with the *growth* of voidage instabilities, since in liquid-fluidized beds these instabilities do not grow into discrete bubbles. The aim of magnetic stabilization in MSFB chromatography is to prevent axial particle mixing, so it may be more appropriate to examine the stability of the uniform fluidized state with respect to solids phase velocity perturbations. Unfortunately, no simple analytical solution of the type demonstrated herein for voidage instabilities seems to exist for particle velocity perturbations, since the perturbed fluid equation of continuity (Eq. 1') cannot be expressed entirely in terms of particle velocity. Homsy (1983) surveyed some results in the theory of fluidization, including the case of magnetic stabilization, and concluded that the theory was in a primitive state relative to more established areas of fluid mechanics and that solutions to (nontrivial) nonlinear problems were yet to be developed. It is beyond the scope of this article to examine this aspect in more detail, but it may be worth pursuing in future work.

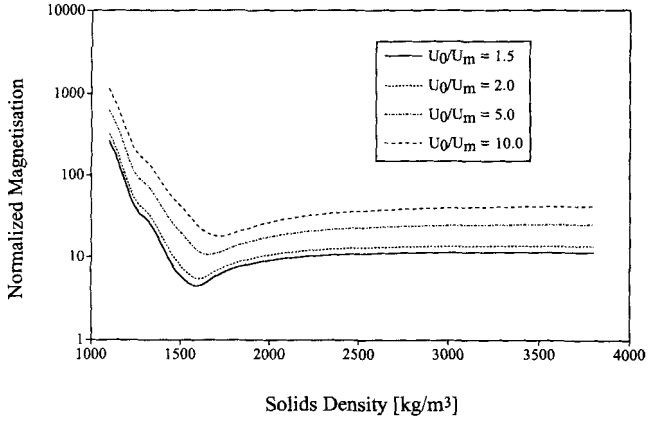

Figure 2. Magnetization required to achieve neutral stability as a function of solids phase density for a water-fluidized bed; fluid density is 1,000 kg/m³.

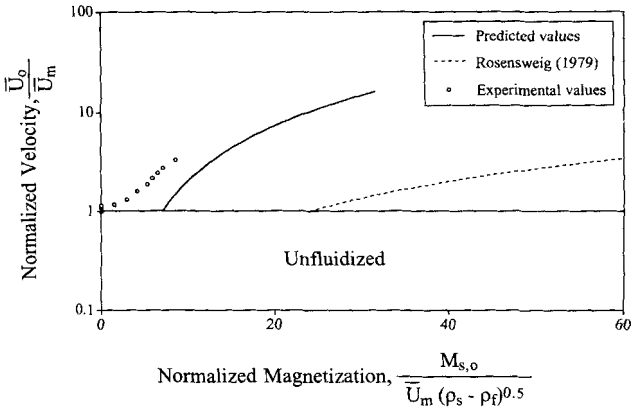

Figure 3. Stability diagram for CAM beads.

$C(\epsilon) = 0.5$, $\epsilon_d = 0.42$, $\rho_s = 1{,}800$ kg/m³, $\hat{\chi} = 2.4\times10^{-7}$ Wb/A m, $\rho_f = 1{,}000$ kg/m³. Experimental values from Cocker (1994).

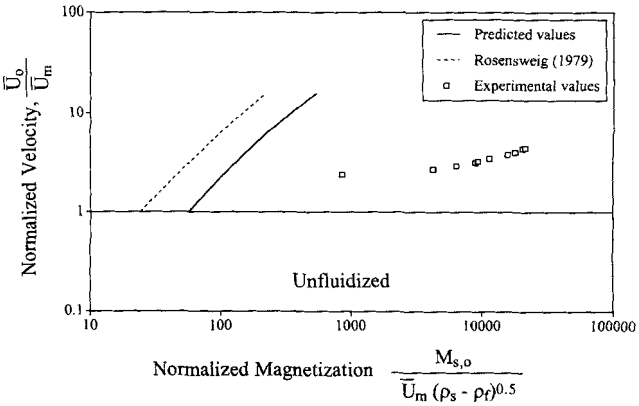

Figure 4. Stability diagram for PAM beads.

$C(\epsilon) = 0.5$, $\epsilon_d = 0.39$, $\rho_s = 1{,}200$ kg/m³, $\hat{\chi} = 8.5\times10^{-7}$ Wb/A m, $\rho_f = 1{,}000$ kg/m³. Experimental values from Cocker (1994).

Conclusions

The MSFB stability analysis of Rosensweig (1979) has been extended to include terms dependent on the fluid density. The normalized magnetization, used in a stability diagram to show a curve of neutral stability at given values of the normalized superficial velocity, contains a term involving the difference in density between the solids and fluid phases, rather than the solids phase density alone.

Comparisons of predicted values with experimentally determined values for the magnetization required for neutral stability show reasonable agreement for CAM beads but unacceptable differences for PAM beads. Although the values predicted from this analysis lie closer to the experimental values than those predicted by Rosensweig, the theory still cannot quantitatively predict actual stability behavior, at least for the case of a solids phase density that is relatively close to the fluid phase density.

Further work should be aimed at achieving a quantitatively predictive model of stability for use in assessing new magnetically susceptible chromatography resins and algorithms for control of magnetic field strength in actual MSFB chromatography columns, with the focus on the growth of perturbations from the steady-state solution for uniform fluidization with respect to particle velocity rather than voidage.

Notation

$\boldsymbol{B}$ = magnetic induction vector, Wb/m^2
$\boldsymbol{B}_1$ = pertubation of magnetic induction vector, Wb/m^2
$C(\epsilon)$ = a virtual mass coefficient
$C_o' = \partial C/\partial\epsilon \mid_{\epsilon=\epsilon_o+\epsilon_1}$
$\boldsymbol{E}$ = fluid stress tensor, Pa
$\boldsymbol{E}^s$ = solids stress tensor, Pa
$\boldsymbol{E}^m$ = magnetic stress tensor, Pa
$\boldsymbol{f}$ = particle-to-fluid drag force per unit volume, Pa/m
$\boldsymbol{f}_m$ = magnetic body force, Pa/m
$\boldsymbol{g}$ = vector acceleration of gravity, m/s^2
g = magnitude of the vector acceleration of gravity, m/s^2
$\boldsymbol{H}$ = magnetic field vector, A/m
H = magnitude of magnetic field, A/m
H_o = magnitude of magnetic field under steady-state uniform conditions, A/m
$\boldsymbol{H}_1$ = perturbation of magnetic field vector, A/m
K = constant in Carman–Kozeny relation, Pa·s/m^2
$\boldsymbol{M}$ = vector magnetization of bed medium, Wb/m^2
M = magnitude of magnetization for the bed medium, Wb/m^2
M_o = magnitude of magnetization under steady-state uniform conditions, Wb/m^2
$\boldsymbol{M}_1$ = perturbation of vector magnetization of bed medium, Wb/m^2
M_s = magnitude of magnetization for bed solids, Wb/m^2
$M_{s,o}$ = magnitude of magnetization for the bed solids in the uniform bed, Wb/m^2
p = pressure, Pa
p_o = magnitude of pressure under steady-state uniform conditions, Pa
p_1 = perturbation of pressure, Pa
t = time, s
$\boldsymbol{u}$ = fluid velocity vector, m/s
$\bar{u}_{mf}$ = superficial velocity of the fluid at the point of minimum fluidization, m/s
u_o = magnitude of fluid velocity under steady-state uniform conditions, m/s
$\boldsymbol{u}_1$ = perturbation of fluid velocity, m/s
$\boldsymbol{v}$ = particle velocity vector, m/s
$\boldsymbol{v}_1$ = perturbation of particle velocity vector, m/s

Greek letters

$\beta(\epsilon, M)$ = a drag coefficient for particle to fluid, Pa·s/m^2
β_o = the value of $\beta(\epsilon)$ at $\epsilon = \epsilon_o$
$\beta_o' = \partial\beta/\partial\epsilon \mid_{\epsilon=\epsilon_o+\epsilon_1}$
ϵ = void fraction of bed
ϵ_o = magnitude of voidage under steady-state uniform conditions
ϵ_1 = perturbation of voidage
μ = fluid viscosity, N·s/m^2
μ_o = permeability of free space = $4\pi \times 10^{-7}$ Wb/A·m
ρ_f = fluid density, kg/m^3
ρ_s = particle density, kg/m^3
χ_o = chord susceptibility, Wb/A·m
$\hat{\chi}$ = differential susceptibility, the tangent to the curve in a plot of M vs. H, Wb/A·m

Literature Cited

Anderson, T. B., and R. Jackson, "Fluid Mechanical Description of Fluidized Beds: Stability of the State of Uniform Fluidization," *Ind. Eng. Chem. Fundam.*, **7**, 12 (1968).

Burns, M. A., G. I. Kvesitadze, and D. J. Graves, "Dried Calcium Alginate/Magnetite Spheres: A New Support for Chromatographic Separations and Enzyme Immobilization," *Biotechnol. Bioeng.*, **28**, 137 (1985).

Cocker, T. M., "Preparation of Magnetically Susceptible Chromatography Beads for Use in Magnetically Stabilized Fluidized Beds," M.S. Thesis, Univ. of Waikato, Hamilton, New Zealand (1994).

Goetz, V., M. Remaud, and D. J. Graves, "A Novel Magnetic Silica Support for Use in Chromatographic and Enzymatic Bioprocessing," *Biotechnol. Bioeng.*, **37**, 614 (1991).

Graves, D. J., "Bioseparations in the Magnetically Stabilized Fluidized Bed," *Chromat. Sci.*, **61**, 187 (1993).

Homsy, G. M., "A Survey of Some Results in the Mathematical Theory of Fluidization," *Theory of Dispersed Multiphase Flow*, R. E. Meyer, ed., Academic Press, New York, 57 (1983).

Lochmüller, C. H., L. S. Wigman, and B. S. Kitchell, "Aerosol-Jet Produced, Magnetic Carrageenan-Gel Particles: A New Affinity Chromatography Matrix," *J. Chem. Tech. Biotech.*, **40**, 33 (1987).

Rosensweig, R. E., "Magnetic Stabilization of the State of Uniform Fluidization," *Ind. Eng. Chem. Fundam.*, **18**, 260 (1979).

Rosensweig, R. E., and G. Ciprios, "Magnetic Liquid Stabilization in a Bed of Nonmagnetic Spheres," *Powder Technol.*, **64**, 115 (1991).

Richardson, J. F., and W. N. Zaki, "Sedimentation and Fluidization: 1," *Trans. Ind. Chem. Eng.*, **32**, 35 (1954).

Sacj, L. M., Z. R. Jovanovic, G. Vunjak-Novakovic, R. D. Pesic, and D. V. Vukovic, "Liquid Dispersion in a Magnetically Stabilized Fluidized Bed (MSFB)," *Trans. Ind. Chem. Eng.*, **72**, 236 (1994).

Siegell, J. H., "Magnetized Fluidized Beds," *Powder Technol.*, **64**, 1 (1991).

Tien, C., private communication (1993).

Manuscript received Feb. 8, 1995, and revision received Aug. 14, 1995.